

Epidemic spreading and immunization with identical infectivity

Rui Yang¹, Jie Ren², Wen-Jie Bai¹, Tao Zhou^{1,2,*}, Ming-Feng Zhang¹, and Bing-Hong Wang¹

¹*Department of Modern Physics and Nonlinear Science Center,*

University of Science and Technology of China, Hefei 230026, P. R. China

²*Department of Physics, University of Fribourg, CH-1700 Fribourg, Switzerland*

(Dated: July 18, 2018)

In this paper, a susceptible-infected-susceptible (SIS) model with identical infectivity, where each node is assigned with the same capability of active contacts, A , at each time step, is presented. We found that on scale-free networks, the density of the infected nodes shows the existence of threshold, whose value equals $1/A$, both demonstrated by analysis and numerical simulation. The infected population grows in an exponential form and follows hierarchical dynamics, indicating that once the highly connected hubs are reached, the infection pervades almost the whole network in a progressive cascade. In addition, the effects of random, proportional, and targeted immunization for this model are investigated. Based on the current model and for heterogenous networks, the targeted strategy performs best, while the random strategy is much more efficient than in the standard SIS model. The present results could be of practical importance in the setup of dynamic control strategies.

PACS numbers: 89.75.Hc, 87.23.Ge, 87.19.Xx, 05.45.Xt

I. INTRODUCTION

Epidemic, one of the most important issues related to our real lives, such as computer virus on Internet and venereal disease on sexual contact networks, attracts a lot of attention. Among all the models on the process of the epidemic, susceptible-infected (SI) model [1, 2], susceptible-infected-susceptible (SIS) model [3, 4], and susceptible-infected-removed (SIR) model [5, 6, 7], are considered as the theoretical templates since they can, at least, capture some key features of real epidemics. After some classical conclusions have been achieved on regular and random networks, recent studies on small-world (SW) networks [8] and scale-free (SF) networks [9] introduce fresh air into this long standing area (see the reviews [10] and the references therein). The most striking result is that in the SIS and SIR model, the critical threshold vanishes in the limit of infinite-size SF networks. It is also a possible explanation why some diseases are able to survive for a long time with very low spreading rate.

In this paper, we focus on the SIS model. Although it has achieved a big success, the standard SIS style might contain some unexpected assumption while being introduced to the SF networks directly, that is, each node's potential infection-activity (infectivity), measured by its possibly maximal contribution to the propagation process within one time step, is strictly equal to its degree. As a result, in the SF networks the nodes with large degree, named *hubs*, will take the greater possession of the infectivity, so-called *super-spreader*. This assumption may fail to mimic some cases in the real world where the relation between degree and infectivity is not simply equal [11]. The first example is that, in most of the existing peer-to-peer distributed systems, although

their long-term communicating connectivity shows the scale-free characteristic [12], all peers have identical capabilities and responsibilities to communicate at a short term, such as the Gnutella networks [13]. Second, in sexual contact networks, even the hub node has many acquaintances; he/she has limited capability to contact with others during limited periods [14]. Third, the referral of a product to potential consumers costs money and time in network marketing processes (e.g. a salesman has to make phone calls to persuade his social surrounding to buy the product). Therefore, the salesman will not make referrals to all his acquaintances [15]. The last one, in some email service systems, such as the Gmail system schemed out by Google [16], the clients are assigned by limited capability to invite others to become Gmail-user after being invited by an E-mail from another Gmail-user. Similar phenomena are common in our daily lives, thus need a further investigation.

II. THE MODEL

In the epidemic contact network, node presents individual and link denotes the potential contacts along which infections can spread. Each individual can be in two discrete states, whether susceptible (S) or infected (I). At each time step, the susceptible node which is connected to the infected one will be infected with rate β . Meanwhile, infected nodes will be cured to be again susceptible with rate δ , defining the effective spreading rate as $\lambda = \beta/\delta$. Without losing of generality, we set $\delta = 1$. Individuals run stochastically through the cycle susceptible-infected-susceptible, which is also the origin of the name, SIS. Denote $S(t)$ and $I(t)$ the density of the susceptible and infected population at the time step t , respectively. Then

$$I(t) + S(t) = 1. \quad (1)$$

*Electronic address: zhutou@ustc.edu

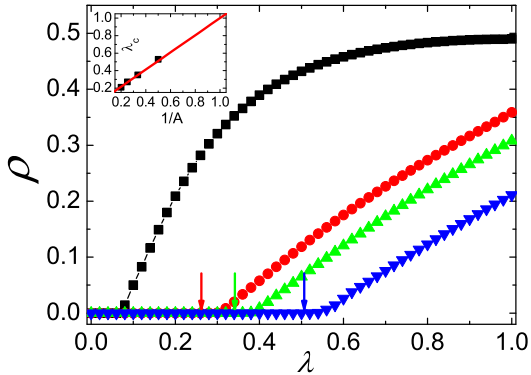


FIG. 1: (Color online) Average value of ρ as a function of the effective spreading rate λ on a BA network with average degree $\langle k \rangle = 8$ and network size $N = 2000$. The black points represent the case of standard SIS model, and the red, green and blue points correspond to the present model with $A = 4, 3$ and 2 , respectively. The arrows point at the critical points gained from the simulation. The insert shows the threshold λ_c scaling with $1/A$, with solid line representing the analytical results.

In the standard SIS model, each individual will contact all its neighbors once at each time step, thus the infectivity of each node is equal to its degree. In the present model, we assume that every individual has the same infectivity A . That is to say, at each time step, each infected individual will generate A contacts where A is a constant. Multiple contacts to one neighbor are allowed, and the contacts to the infected ones, although without any effect on the epidemic dynamics, are also counted. In this paper, with half nodes infected initially, we run the spreading process for sufficiently long time, and calculate the fraction of infected nodes averaging over the last 1000 steps as the density of infected nodes in the steady stage (denoted by ρ). All of our simulation results are obtained from averaging over 300 different network realizations, and for each 100 independent runs with different initial configurations.

III. THRESHOLD BEHAVIOR

Let $I_k(t)$ denote the fraction of vertices of degree k that are infected at time t . Then using the mean-field approximation, the rate equation for the partial densities $I_k(t)$ in a network characterized by a degree distribution $P(k)$ can be written as:

$$\partial_t I_k(t) = -I_k(t) + \lambda k [1 - I_k(t)] \sum_{k'} \frac{P(k'|k) I_{k'}(t) A}{k'}, \quad (2)$$

where $P(k'|k)$ denotes the conditional probability that a vertex of degree k is connected to a vertex of degree k' .

Considered the uncorrelated networks, where $P(k'|k) = k' P(k') / \langle k \rangle$, the rate equation takes the form:

$$\partial_t I_k(t) = -I_k(t) + \lambda \frac{k}{\langle k \rangle} [1 - I_k(t)] I(t) A. \quad (3)$$

Using ρ_k to denote the value of $I_k(t)$ in the steady stage with sufficiently large t , then

$$\partial_t \rho_k = 0, \quad (4)$$

which yields the nonzero solutions

$$\rho_k = \frac{\lambda k \rho A / \langle k \rangle}{1 + \lambda k \rho A / \langle k \rangle}, \quad (5)$$

where $\rho = \sum_k P(k) \rho_k$ is the infected density at the network level in the steady stage. Then, one obtains

$$\rho = \frac{\lambda \rho A}{\langle k \rangle} \sum_k \frac{k P(k)}{1 + \lambda k \rho A / \langle k \rangle}. \quad (6)$$

To the end, for the critical point where $\rho \sim 0$, we get

$$\lambda A = \frac{\langle k \rangle}{\sum_k k P(k)} = 1. \quad (7)$$

This equation defines the epidemic threshold

$$\lambda_c = \frac{1}{A}, \quad (8)$$

below which the epidemic prevalence is null, and above which it attains a finite value. The previous works about epidemic spreading in SF networks present us with a completely new scenario that a highly heterogeneous structure will lead to the absence of any epidemic threshold [10], while now, in the present model, it is $1/A$ instead. As shown in Fig. 1, the analytical result agrees very well with the simulations. Furthermore, it is also clear that the larger infectivity A will lead to the higher prevalence ρ .

From the analytical result of the threshold value, $\lambda_c = 1/A$, we can also acquire that the critical behavior is independent of the topology of networks which are valid for the mean-field approximation [17]. To demonstrate this proposition, we implement the present model on various networks; These include the random networks, the scale-free configuration model [18] with different power-law exponent γ , and the BA networks with different average degree. As shown in Fig. 2, under a given A , the critical value are the same, which strongly support the valid of Eq. (8). Furthermore, there is no distinct finite-size effect as shown in Fig. 3. In the original SIS model, the node's infectivity relies strictly on its degree k and the threshold is $\lambda_c \sim \langle k \rangle / \langle k^2 \rangle$. Since the variance of degrees gets divergent with the increase of N , the epidemic propagation on scale-free networks has an obvious size effect [19]. However, in the current model, each infected node is just able to contact the same number of neighbors, A , rather than its degree. Thus the threshold value and the infected density beyond the threshold are both independent of the size N .

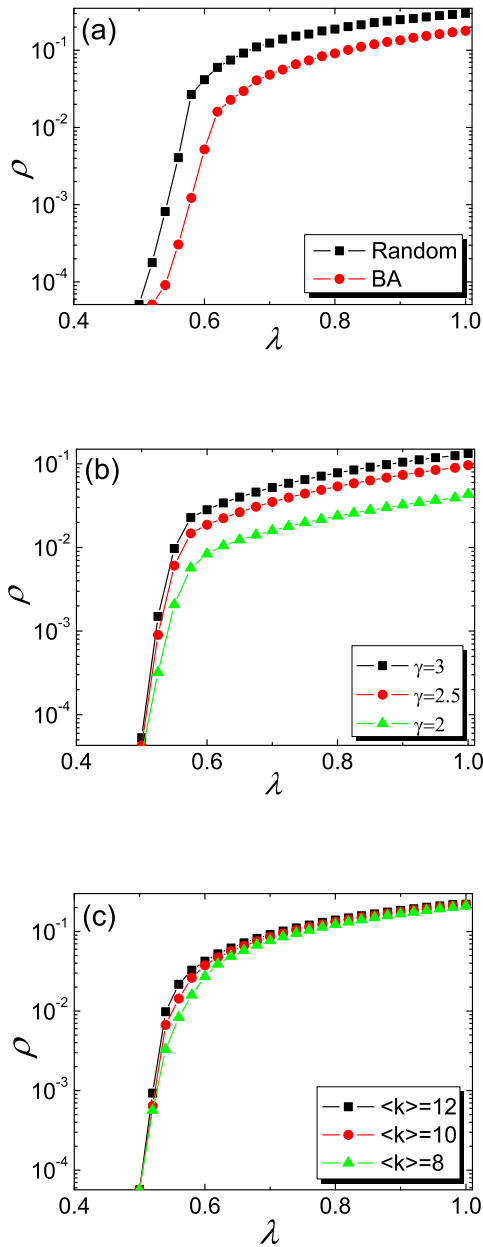


FIG. 2: (Color online) Average value of ρ as a function of the effective spreading rate λ on (a) the random and BA networks; (b) the SF configuration networks for different values of γ ; (c) the BA networks with different average degree. In (a) and (b), the average degree is with $\langle k \rangle = 6$, and for all the simulations, $N = 2000$ and $A = 2$ are fixed.

IV. TIME BEHAVIOR

For further understanding of the epidemic dynamics of the proposed model, we study the time behavior of the epidemic propagation. First of all, manipulating the operator $\sum_k P(k)$ on both sides of Eq. (3), and neglecting

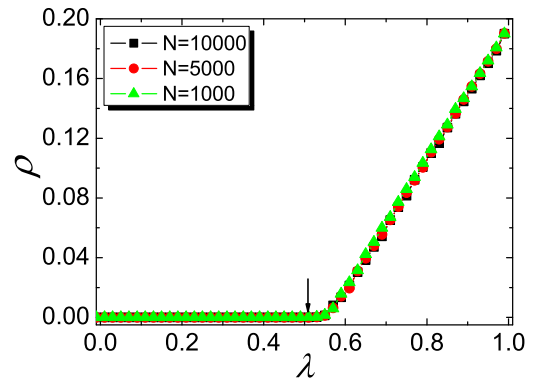


FIG. 3: (Color online) Average value of ρ as a function of the effective spreading rate λ on the different sizes of BA networks with $\langle k \rangle = 6$ and $A = 2$.

the terms of order $\mathcal{O}(I^2)$, we obtain

$$\partial_t I(t) = -I(t) + \lambda AI(t). \quad (9)$$

Thus the evolution of $I(t)$ follows an exponential growing as

$$I(t) \sim e^{ct}, \quad (10)$$

where $c \propto (\lambda A - 1)$.

In Fig. 4, we report the simulation results of the present model for different spreading rates ranging from 0.7 to 0.9. The rescaled curves $I(t)/I(t)_{max}$ (Fig. 4(b)) can be well fitted by a straight line in single-log plot for small t and the curves corresponding to different λ will collapse to one curve with rescaling time $(\lambda A - 1)t$, which strongly supports the analytical result Eq. (10).

Furthermore, a more precise characterization of the epidemic diffusion through the network can be achieved by studying some convenient quantities in numerical experiments. First, we measure the average degree of newly infected nodes at time t as

$$\langle k_{inf}(t) \rangle = \frac{\sum_k k I_k(t)}{I(t)}. \quad (11)$$

Then, we present the inverse participation ratio $Y_2(t)$ to indicate the detailed information on the infection propagation, which is defined as [20]:

$$Y_2(t) = \sum_k w_k^2(t), \quad (12)$$

where the weight of recovered individuals in each k -degree class (here k -degree class means the set of all the nodes with degree k) is defined by $w_k(t) = I_k(t)/I(t)$. From this definition, one can acquire that if Y_2 is small, the infected are homogeneously distributed among all degree classes; on the contrary, if Y_2 is relatively larger then, the infection is localized on some specific degree classes.

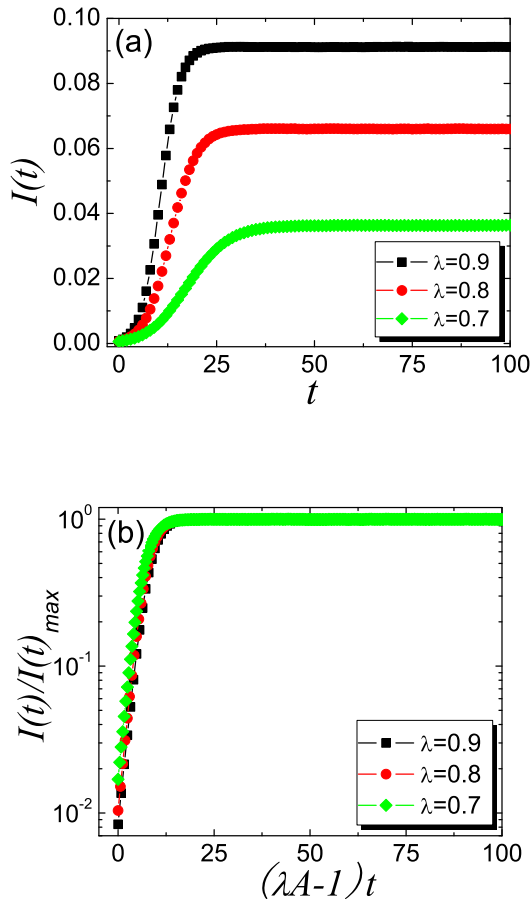


FIG. 4: (Color online) Average value of $I(t)$ in normal plots as time t (a) and $I(t)/I(t)_{max}$ in single-log plots as rescaled time $(\lambda A - 1)t$ (b) for different spreading rate λ . The numerical simulations are implemented based on BA networks of size $N = 2000$, $\langle k \rangle = 6$, and $A = 2$.

In Fig. 5, we exhibit the time behaviors of these quantities for BA networks and find a hierarchical dynamics, that is, all those curves show an initial plateau, which denotes that the infection takes control of the large degree nodes firstly. Once the highly connected hubs are reached, the infection pervades almost the whole network via a hierarchical cascade across smaller degree classes. Thus, $\langle k_{inf}(t) \rangle$ decreases to the next plateau, which approximates the average degree $\langle k \rangle$.

V. IMMUNIZATION

Immunity, relating to the people's strategies to struggle with the disease epidemics, shows great importance in practice [10]. Since the current model, which can mimic some real cases more accurately, shows different characters with the standard SIS model, it requires some

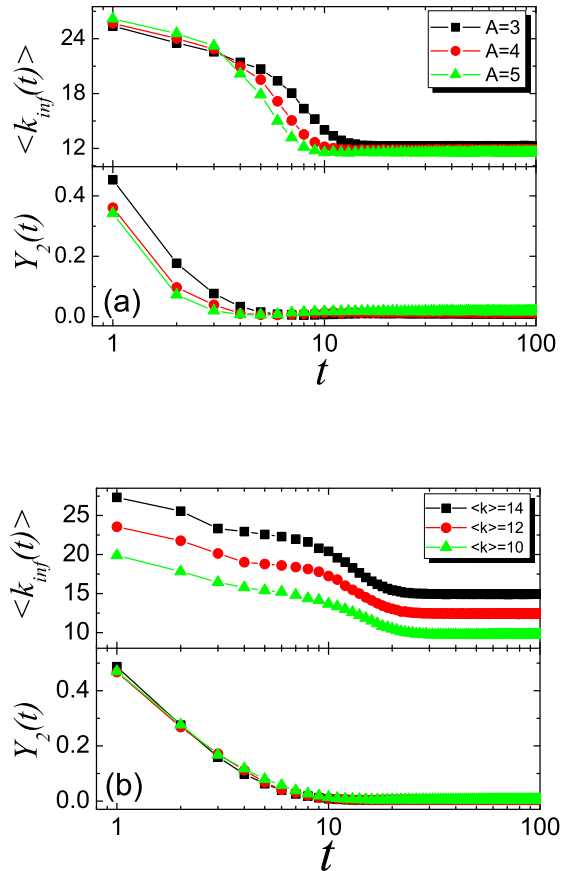


FIG. 5: (Color online) Time behavior of the average degree of the newly infected nodes (top) and inverse participation ratio Y_2 (bottom) in BA networks of size $N = 2000$, $\lambda = 0.8$ for different values of A (with $\langle k \rangle = 12$ fixed) (a) and $\langle k \rangle$ (with $A = 2$ fixed) (b).

in-depth and detailed investigation about the immunity on this model. As we know, immunized nodes cannot become infected and, therefore, will not transmit the infection to their neighbors. The simplest immunization strategy is to select immunization population completely randomly, so-called *random immunization* [21]. However, this strategy is inefficient for heterogenous networks. Similar to the preferential attachment mechanism introduced by BA model [9], Dezső and Barabási proposed the *proportional immunization* strategy [22], in which the immunizing probability of each node is proportional to its degree. This preferential selection strategy can remarkable enhance the immunization efficiency in scale-free networks. The extreme strategy for immunization in heterogenous networks is the so-called *targeted immunization* [23], where the most highly connected nodes are chosen to be immunized. Compared with the random immunization and proportional immunization, the targeted immunization is demonstrated as the most effi-

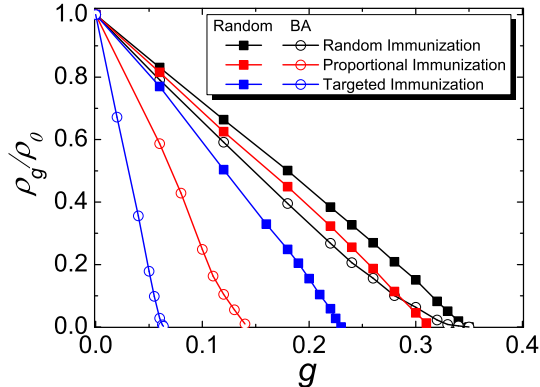


FIG. 6: (Color online) Reduced prevalence ρ_g/ρ_0 from numerical simulations of the present model in the random (square point) and BA (circle point) network with random (black line), proportional (red line) and targeted immunizations (blue line). In the simulations, the parameter $\lambda = 0.8$, $A = 2$, $\langle k \rangle = 6$ and $N = 2000$ are fixed.

cient one for various networks [24], and several different but relative dynamics [25].

In Fig. 6, we report the simulation results about the three mentioned immunization strategies on the current model. The x -axis, g , denotes the fraction of immunized population, and the y -axis, ρ_g/ρ_0 , represents the performance, where ρ_0 is the prevalence of infected nodes without immunization and ρ_g the one after immunization. From the simulation results, one can find that the epidemic thresholds under random, proportional and targeted immunizations of random networks are $g_c \simeq 0.35$, 0.32 and 0.23 , respectively. And those of BA networks are $g_c \simeq 0.35$, 0.14 and 0.07 . It is clear from the simulation results, even in the current model where the infectivities of large-degree nodes are greatly suppressed, the targeted immunization performs best. Combine with the hierarchical behavior observed in Sec. IV, it strongly indicates that the heterogeneities of degree and infectivity could both contribute to the violent spreading of disease. Hence even for the current model with identical infectivity, the hub nodes play much more important roles in determining the dynamical property.

Note that, in this model, for heterogenous networks, the random immunization is more efficient than the standard case, and the threshold g_c is the same for BA and random networks. Actually, the random immunization is implemented by randomly selecting and immunizing gN nodes on a network of fixed size N . At the mean-field level, the presence of uniform immunity will effectively reduce the spreading rate λ by a factor $(1 - g)$. According to Eq. (8), the immunization threshold is given by

$$g_c = 1 - \frac{1}{A\lambda}. \quad (13)$$

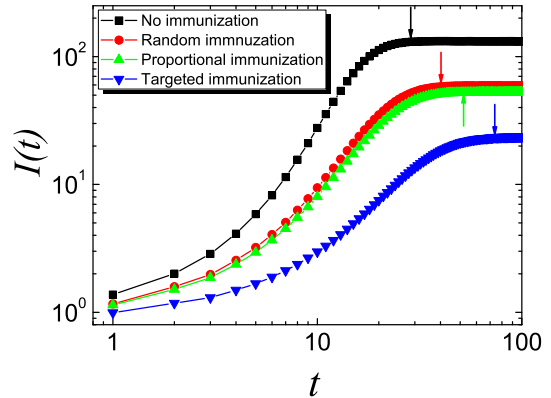


FIG. 7: (Color online) Average value of $I(t)$ as time t for no immunization (black), random immunization (red), proportional immunization (green), and targeted immunization (blue) at $\lambda = 0.8$ and $g = 0.01$. The numerical simulations are implemented based on BA networks of size $N = 2000$, $\langle k \rangle = 6$, and $A = 2$. The arrows indicate the time that the whole spreading process comes to the steady stage.

As shown in Fig. 6, the simulated result ($g_c \simeq 0.35$) agrees with the analytical result ($g_c = 0.375$) well. To compare, the random immunization threshold of standard SIS model is given by $g_c = 1 - \langle k \rangle / \lambda \langle k^2 \rangle$ [23]. Namely, to control the spreading, one have to immunize all the population as $g_c(N) \rightarrow 1$ in the thermodynamic limit $N \rightarrow \infty$.

For further understanding the effects of those different immunization strategies, we study the time behaviors as shown in Fig. 7. In accordance with the above results, the spreading velocity under target immunization is the lowest. Note that, different from the standard SIS model, the random immunization can obviously slow down the spreading in the early stage even with a tiny population $g \sim 1\%$.

VI. CONCLUSION

In this paper, we investigated the behaviors of SIS epidemics with the identical infectivity A . By comparing the dynamical behaviors of the present model of different values of A with the standard one on BA networks, we found the existence of epidemic spreading threshold. The analytical result of the threshold $1/A$ is provided, which agrees with numerical simulation very well. The critical value is independent of the topology of underlying networks, just depends on the dynamical parameter A and the whole spreading process does not have the distinct finite-size effect. For SF networks, the infected population grows in an exponential form in the early stage, and then follows a hierarchical dynamics. In addition, the

time scale is also independent of the underlying topology.

The last but not the least, the numerical results of random, proportional, and targeted immunization are presented. We found that the targeted immunization performs best, while the random immunization is much more efficient in heterogenous networks than the standard case.

Acknowledgments

BHWang acknowledges the support of 973 Project under Grant No. 2006CB705500, the Special Research

Founds for Theoretical Physics Frontier Problems under Grant No. A0524701, the Specialized Program under the Presidential Funds of the Chinese Academy of Science, and the National Natural Science Foundation of China under Grant No. 10472116. TZhou acknowledges the support of the National Natural Science Foundation of China under Grant Nos. 70471033 and 10635040.

-
- [1] M. Barthélemy, A. Barrat, R. Pastor-Satorras, and A. Vespignani, *Phys. Rev. Lett.* **92**, 178701 (2004); M. Barthélemy, A. Barrat, R. Pastor-Satorras, and A. Vespignani, *J. Theor. Biol.* **235**, 275 (2005).
- [2] T. Zhou, G. Yan, and B. -H. Wang, *Phys. Rev. E* **71**, 046141 (2005); G. Yan, T. Zhou, J. Wang, Z. -Q. Fu, and B. -H. Wang, *Chin. Phys. Lett.* **22**, 510 (2005).
- [3] R. Pastor-Satorras and A. Vespignani, *Phys. Rev. Lett.* **86**, 3200 (2001); R. Pastor-Satorras and A. Vespignani, *Phys. Rev. E* **63**, 066117 (2001).
- [4] M. Boguñá, and R. Pastor-Satorras, *Phys. Rev. E* **66**, 047104 (2002); M. Boguñá, R. Pastor-Satorras, and A. Vespignani, *Phys. Rev. Lett.* **90**, 028701 (2003).
- [5] R. M. May and A. L. Lloyd, *Phys. Rev. E* **64**, 066112 (2001); A. L. Lloyd, and R. M. May, *Science* **292**, 1316 (2001).
- [6] Y. Moreno, R. Pastor-Satorras and A. Vespignani, *Eur. Phys. J. B* **26**, 521 (2002); Y. Moreno, J. B. Gomez, and A. F. Pacheco, *Phys. Rev. E* **68**, 035103 (2003).
- [7] G. Yan, Z. -Q. Fu, J. Ren, W. -X. Wang, *Phys. Rev. E* **75**, 016108 (2007).
- [8] D. J. Watts and S. H. Strogats, *Nature (london)* **393**, 440 (1998).
- [9] A.-L. Barabási and R. Albert, *Science* **286**, 509 (1999).
- [10] R. Pastor-Satorras, and A. Vespignani, *Epidemics and immunization in scale-free networks*. In: S. Bornholdt, and H. G. Schuster (eds.) *Handbook of Graph and Networks*, Wiley-VCH, Berlin, 2003; T. Zhou, Z. -Q. Fu, and B. -H. Wang, *Prog. Nat. Sci.* **16**, 452 (2006); S. Boccaletti, V. Latora, Y. Moreno, M. Chavez, and D. -U. Hwang, *Phys. Rep.* **424**, 175 (2006).
- [11] J. Joo, and J. L. Leboitz, *Phys. Rev. E* **69**, 066105 (2004); R. Olinky, and L. Stone, *Phys. Rev. E* **70**, 030902 (2004); T. Zhou, J.-G. Liu, W.-J. Bai, G.-R. Chen, and B.-H. Wang, *Phys. Rev. E* **74**, 056109 (2006); R. Yang, B.-H. Wang, J. Ren, W.-J. Bai, Z.-W. Shi, W.-X. Wang, and T. Zhou, *Phys. Lett. A* **364**, 189 (2007).
- [12] M. A. Jovanovic, *Modeling large-scale peer-to-peer networks and a case study of Gnutella* [M.S. Thesis], University of Cincinnati (2001).
- [13] [Http://www.gnutella.com](http://www.gnutella.com).
- [14] F. Liljeros, C. R. Edling, L. A. N. Amaral, H. E. Stanley, and Y. Åberg, *Nature* **411**, 907 (2001); W. -J. Bai, T. Zhou, and B. -H. Wang, *Int. J. Mod. Phys. C* (to be published).
- [15] B. J. Kim, T. Jun, J. Y. Kim, and M. Y. Choi, *Physica A* **360**, 493 (2005).
- [16] [Http://mail.google.com/mail/help/intl/en/about.html](http://mail.google.com/mail/help/intl/en/about.html).
- [17] Note that, if the connections of the underlying networks are localized (e.g. lattices), then the mean-field approximation is incorrect and the threshold value is not equal to $1/A$.
- [18] M. Molloy, and B. Reed, *Random Struct. Algorithms* **6**, 161 (1996); M. Molloy, and B. Reed, *Combinatorics, Probab. Comput.* **7**, 295 (1998).
- [19] R. Pastor-Satorras and A. Vespignani, *Phys. Rev. E* **65**, 035108 (2002); D. -U. Hwang, S. Boccaletti, Y. Moreno, and R. Lopez-Ruiz, *Math. Biosci. & Eng.* **20**, 317 (2005).
- [20] B. Derrida and H. Flyvbjerg, *J. Phys. A* **20** 5273 (1987).
- [21] J. Müller, *SIAM J. Appl. Math.* **59**, 222 (1998); D. S. Callaway, M. E. J. Newman, S. H. Strogatz, and D. J. Watts, *Phys. Rev. Lett.* **85**, 5468 (2000); R. Cohen, K. Erez, D. ben-Avraham, and S. Havlin, *Phys. Rev. Lett.* **85**, 4626 (2000).
- [22] Z. Dezsö, and A.-L. Barabási, *Phys. Rev. E* **65**, 055103 (2002).
- [23] R. Pastor-Satorras and A. Vespignani, *Phys. Rev. E* **65**, 036104 (2002).
- [24] Z. H. Liu, Y. C. Lai, and N. Ye, *Phys. Rev. E* **67**, 031911 (2003); D. H. Zanette, and M. Kuperman, *Physica A* **309**, 445 (2002); Y. C. Lai, Z. H. Liu, and N. Ye, *Int. J. Mod. Phys. B* **17**, 4045 (2003); H. Zhang, Z. H. Liu, and W. C. Ma, *Chin. Phys. Lett.* **23**, 1050 (2006).
- [25] N. Madar, T. Kalisky, R. Cohen, D. ben-Avraham, and S. Havlin, *Eur. Phys. J. B* **38**, 269 (2004); T. Zhou, and B. -H. Wang, *Chin. Phys. Lett.* **22**, 1072 (2005); F. Takeuchi, and K. Yamamoto, *Lect. Notes Comput. Sci.* **3514**, 956 (2005); W. -J. Bai, T. Zhou, and B. -H. Wang, arXiv: physics/0610138.